Mechanics of hemispherical electronics

Shuodao Wang,[1] Jianliang Xiao,[1] Inhwa Jung,[2] Jizhou Song,[3] Heung Cho Ko,[4] Mark P. Stoykovich,[5] Yonggang Huang,[1,6,a)] Keh-Chih Hwang,[7] and John A. Rogers[2,8,a)]
[1]*Department of Mechanical Engineering, Northwestern University, Evanston, Illinois 60208, USA*
[2]*Department of Materials Science and Engineering, University of Illinois, Urbana, Illinois 61801, USA*
[3]*Department of Mechanical and Aerospace Engineering, University of Miami, Coral Gables, Florida 33146, USA*
[4]*Department of Materials Science and Engineering, Gwangju Institute of Science and Technology (GIST), Gwangju 500-712, Republic of Korea*
[5]*Department of Chemical and Biological Engineering, University of Colorado-Boulder, Boulder, Colorado 80309, USA*
[6]*Department of Civil and Environmental Engineering, Northwestern University, Evanston, Illinois 60208, USA*
[7]*Department of Engineering Mechanics, Tsinghua University, Beijing 100084, China*
[8]*Department of Chemistry and Department of Mechanical Science and Engineering, University of Illinois, Urbana, Illinois 61801, USA*

(Received 27 August 2009; accepted 1 October 2009; published online 5 November 2009)

A simple analytical model is established for the development of hemisphere electronics, which has many important applications in electronic-eye cameras and related curvilinear systems. The photodetector arrays, made in planar mesh layouts with conventional techniques, are deformed and transferred onto a hemisphere. The model gives accurately the positions of photodetectors on the hemisphere, and has been validated by experiments and finite element analysis. The results also indicate very small residual strains in the photodetectors. The model provides a tool to define a pattern of photodetectors in the planar, as-fabricated layout to yield any desired spatial configuration on the hemisphere. © *2009 American Institute of Physics*. [doi:10.1063/1.3256185]

Inspired by the remarkable imaging features of the human eye, recent research has examined several different fabrication strategies to form cameras with nonplanar (e.g., hemispherical) photodetector arrays.[1–7] One approach is to transfer silicon devices on a circular plate of polyimide onto a spherical cap.[5] The polyimide substrate is plastically deformed to a hemisphere, and the silicon devices on the substrate are transferred accordingly. This requires change of processing temperature and/or etching of the substrate (underneath interconnects) to accommodate the deformation induced by the transfer. Another approach achieves a working device capable of collecting actual images that validate the optical advantages of a hemispherical layout.[6] Related strategies enable natural integration of electronics with the soft, curvilinear surfaces of living organisms (e.g., human body),[7] which may lead to many important applications such as health monitoring or therapeutics; smart surgical gloves to monitor patients' vital signs; and a curvilinear display that is better suited to the curvature of human eye for gaming.[8] Such curvilinear electronics cannot be achieved by using established materials and processing technologies due to the inherently two-dimensional nature of these procedures, ranging from photolithographic patterning to deposition, etching, and doping.[7]

As illustrated in Fig. 1, this latter approach involves four steps, A, B, C, and D, that transforms planar photodetector arrays into hemispherical ones. The process begins with the formation of a hemispherical, poly(dimethylsiloxane) (PDMS) (Ref. 9) transfer element (radius of curvature ~1 cm), which mounts in a mechanical fixture that provides coordinated radial motion (step A). The radial, elastic deformations in the PDMS transform this hemisphere, at sufficiently large tension, into the planar shape of a 'drumhead' (step B). A matrix focal plane array is then transfer printed[10–12] to the PDMS in its tensioned, planar drumhead shape (step C), and the focal array is weakly bonded to the top surface of PDMS via nonspecific, likely, van der Waals forces. Releasing the radial tension causes the elastomer to relax back, approximately, to its initial hemispherical shape but with a slightly larger radius of curvature (step D). The large strains associated with this process are accommodated by local delamination of narrow, thin interconnects to adopt arc shapes pinned at the ends by the detector pixels.[7]

The uniform, planar photodetectors become nonuniformly distributed on the hemisphere (Step D) due to the nonuniform strain distribution.[6,13–15] This letter establishes a simple analytical model, validated by the finite element

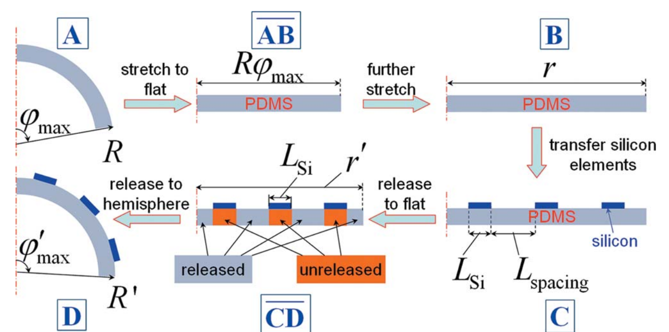

FIG. 1. (Color online) Schematic diagrams of the mechanics model for transferring silicon-based photodetectors from planar arrays onto a hemisphere.

[a)]Authors to whom correspondence should be addressed. Electronic addresses: y-huang@northwestern.edu and jrogers@uiuc.edu.

 © 2009 American Institute of Physics

Downloaded 09 Nov 2009 to 130.126.101.208. Redistribution subject to AIP license or copyright; see http://apl.aip.org/apl/copyright.jsp

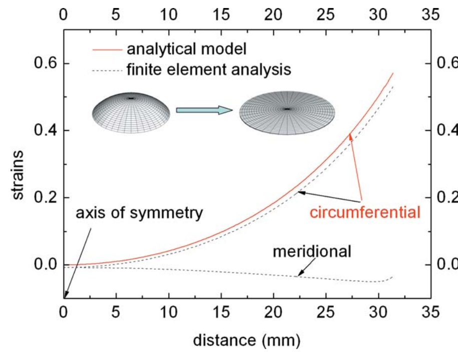

FIG. 2. (Color online) Distribution of meridional and circumferential strains of a PDMS membrane stretched from a hemisphere to a flat "drumhead." The inset shows the initial and deformed meshes.

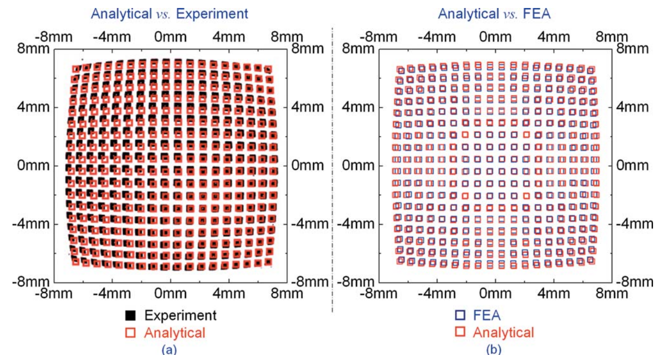

FIG. 3. (Color online) Silicon element positions (top view, measured from the center) given by the analytical model, experiments and finite element analysis.

method, to determine the positions of photodetectors on the hemisphere and the residual strain in photodetectors, which are important to the image quality, and electronic and mechanical performance of photodetectors.

The analytical model (Fig. 1) consists of the aforementioned steps A–D and two intermediate steps $\overline{AB}$ and $\overline{CD}$. Step A shows a cross sectional view of the PDMS hemisphere (radius R and spherical angle $\varphi_{\max}$). The hemisphere is first stretched to a (nearly) flat plate (step $\overline{AB}$), and further to a plate of radius r (step B), onto which the array of photodetectors (silicon elements of size L_{Si} and spacing L_{spacing}) are transferred (step C). The stretch is then released to form a new hemisphere (step D) of spherical angle $\varphi'_{\max}$ and slightly larger radius R', through the intermediate step $\overline{CD}$ that corresponds to the (nearly) flat state. The following analytical model tracks the positions of silicon elements from steps C to D.

From steps A to $\overline{AB}$ the hemisphere is mainly stretched in the circumferential direction such that the strain in the meridional direction is negligibly small, $\varepsilon_{\mathrm{meridional}} \approx 0$. The radius of plate in step $\overline{AB}$ then equals the arc length $R\varphi_{\max}$ of hemisphere. A ring at the spherical angle φ $(0 \leq \varphi \leq \varphi_{\max})$ in step A becomes a ring of radius $R\varphi$ in step $\overline{AB}$, which gives the strain in the circumferential direction, $\varepsilon_{\mathrm{circumferential}} \approx (\varphi - \sin\varphi)/\sin\varphi$. As shown in Fig. 2, this simple analytical solution is verified by the finite element analysis of a hemisphere (radius $R=12.9$ mm, spherical angle $\varphi_{\max}=62.1°$, and thickness varying from 1 mm at the top to about 0.6 mm near the rim). The inset shows the axisymmetric shell elements for the hemisphere and deformed mesh for the stretched circular plate.

The circular plate (radius $R\varphi_{\max}$) in step $\overline{AB}$ is further stretched to the plate of radius r in step B, which imposes uniform circumferential and meridional strains, $(r - R\varphi_{\max})/(R\varphi_{\max})$. A point with the spherical angle φ in step A has the radius $r\varphi/\varphi_{\max}$ in step B, which has also been verified by the finite element analysis.

The photodetector mesh is then transferred onto the top surface of PDMS (Step C). Release of the stretch leads first to a (nearly) flat plate of radius r' in the intermediate step $\overline{CD}$, and then to the hemisphere in step D. Similar to steps A and $\overline{AB}$, the release of stretch from steps $\overline{CD}$ to D is mainly in the circumferential direction such that the strain in the meridional direction is negligibly small, $\varepsilon_{\mathrm{meridional}} \approx 0$. Since the Young's modulus of silicon (130 GPa) (Ref. 16) is five orders of magnitude larger than that of PDMS ($\sim$2 MPa),[9] the stretch in PDMS beneath silicon elements is not released and their size L_{Si} does not change, while the stretch at all other locations is released. Let N denote the number of silicon elements on the PDMS surface (step C) and $f = NL_{\mathrm{Si}}^2/(\pi r^2)$ their area fraction. The average fractions of silicon element length and spacing along any direction are f and $(1-f)$, respectively, such that the radius of the circular plate in the intermediate step $\overline{CD}$ as well as the arc length of new hemisphere in step D are $R'\varphi'_{\max} = r' = fr + (1-f)R\varphi_{\max}$.

The above analysis can also be applied to the circumferential direction; the perimeter $2\pi R' \sin\varphi'_{\max}$ of the hemisphere rim in step D consists of the unreleased part $f \cdot 2\pi r$ underneath silicon elements and the released part $(1-f)\cdot 2\pi R \sin\varphi_{\max}$, i.e., $R' \sin\varphi'_{\max} = fr + (1-f)R \sin\varphi_{\max}$. These yield a simple approximate solution

$$R' = R(1-f)\left(1 + \frac{f}{1-f}\frac{r}{R\varphi_{\max}}\right)^{3/2},$$

$$\varphi'_{\max} = \frac{\varphi_{\max}}{\sqrt{1 + \dfrac{f}{1-f}\dfrac{r}{R\varphi_{\max}}}}. \tag{1}$$

For 18×18 silicon elements with $L_{\mathrm{Si}} = 500$ μm, $R = 12.9$ mm, $\varphi_{\max} = 62.1°$, and $r = 14.8$ mm, Eq. (1) gives the radius $R' = 13.9$ mm and $\varphi'_{\max} = 58.1°$, which agree well with $R' = 13.8$ mm and $\varphi'_{\max} = 55.5°$ obtained from the finite element analysis.

The position each silicon element on the hemisphere is represented by the spherical angle

$$\varphi' = \varphi'_{\max}\frac{r_{\mathrm{pixel}}}{r}, \tag{2}$$

where r_{pixel} is the distance between the element center and the axis of symmetry on the circular plate in Step C. An element with Cartesian coordinates $(x, y, 0)$ on the circular plate in step C moves onto the hemisphere in step D with spherical coordinates $[R', \varphi'_{\max}\sqrt{x^2+y^2}/r, \tan^{-1}(y/x)]$. As shown in Fig. 3(a), this agrees very well ($<2\%$ error) with the top view of element positions determined from experiments, which are obtained by analyzing a top view optical image. Such an image is converted to black and white (binary format). Custom image processing software yields the center of each photodetector pad and returns its position in (x, y) coordinates. The center of each pad is noted as a white

Downloaded 09 Nov 2009 to 130.126.101.208. Redistribution subject to AIP license or copyright; see http://apl.aip.org/apl/copyright.jsp

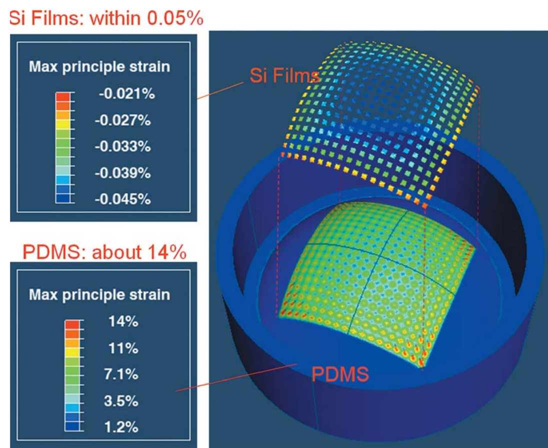

FIG. 4. (Color online) Residual strains in silicon elements and PDMS membrane given by finite element analysis.

dot after the image process. As shown in Fig. 3(b), the analytical results also agree well with the finite element analysis using six-node triangular continuum shell elements for PDMS and four-node conventional shell elements for silicon.

For the same experiment, the finite element analysis gives the maximum principal strain in silicon ~0.05%, which is two orders of magnitude smaller than the strain in PDMS (~14%), as shown in Fig. 4 (Ref. 17). This enables photodetector arrays to be subjected to large (global) strain without failure.

Besides determining the positions of photodetectors on the hemisphere, Eq. (2) also provides a simple way to design nonuniform pattern of such elements on the planar geometry (step C) in order to achieve any desired pattern (e.g., uniform) on the hemisphere (step D). An element with spherical coordinates (R', φ', θ') on the hemisphere in step D has Cartesian coordinates $(r\cos\theta'\varphi'/\varphi'_{max}, r\sin\theta'\varphi'/\varphi'_{max}, 0)$ on the circular plate in step C. The radius and spherical angle of the PDMS transfer element (step A) can be obtained analytically $R=R'[1-fr/(R'\varphi'_{max})]^{3/2}/(1-f)$ and $\varphi_{max}=\varphi'_{max}[1-fr/(R'\varphi'_{max})]^{-1/2}$ from Eq. (1) such that the final hemisphere (step D) has the desired radius R' and spherical angle φ'_{max}.

The authors acknowledge support from NSF (Grant Nos. DMI-0328162 and ECCS-0824129), and DOE, Division of Materials Sciences (Grant No. DE-FG02-07ER46453).

[1]X. Xu, M. Davanco, X. Qi, and S. R. Forrest, Org. Electron. **9**, 1122 (2008).
[2]P. J. Hung, K. Jeong, G. L. Liu, and L. P. Lee, Appl. Phys. Lett. **85**, 6051 (2004).
[3]R. Dinyari, S.-B. Rim, K. Huang, P. B. Catrysse, and P. Peumans, Appl. Phys. Lett. **92**, 091114 (2008).
[4]G. Shin, I. Jung, V. Malyarchuk, J. Song, S. Wang, H. C. Ko, Y. Huang, J. S. Ha, and J. A. Rogers, "Micromechanics and Advanced Designs for Curved Photodetector Arrays in Hemispherical Electronic Eye Cameras," Small (unpublished).
[5]P. I. Hsu, M. Huang, Z. Xi, S. Wagner, Z. Suo, and J. C. Sturm, J. Appl. Phys. **95**, 705 (2004).
[6]H. C. Ko, M. P. Stoykovich, J. Song, V. Malyarchuk, W. M. Choi, C.-J. Yu, J. B. Geddes III, J. Xiao, S. Wang, Y. Huang, and J. A. Rogers, Nature (London) **454**, 748 (2008).
[7]H. C. Ko, G. Shin, S. Wang, M. P. Stoykovich, J. W. Lee, D.-H. Kim, J. S. Ha, Y. Huang, K.-C. Hwang, and J. A. Rogers, "Curvilinear Electronics Formed Using Silicon Membrane Circuits and Elastomeric Transfer Elements," Small (to be published).
[8]S.-I. Park, Y. Xiong, R.-H. Kim, P. Elvikis, M. Meitl, D.-H. Kim, J. Wu, J. Yoon, C.-J. Yu, Z. Liu, Y. Huang, K.-C. Hwang, P. Ferreira, X. Li, K. Choquette, and J. A. Rogers, Science **325**, 977 (2009).
[9]E. A. Wilder, S. Guo, S. Lin-Gibson, M. J. Fasolka, and C. M. Stafford, Macromolecules **39**, 4138 (2006).
[10]Y. Huang, W. Zhou, K. J. Hsia, E. Menard, J.-U. Park, J. A. Rogers, and A. G. Alleyne, Langmuir **21**, 8058 (2005).
[11]X. Feng, M. A. Meitl, A. M. Bowen, Y. Huang, R. G. Nuzzo, and J. A. Rogers, Langmuir **23**, 12555 (2007).
[12]M. A. Meitl, Z.-T. Zhu, V. Kumar, K. J. Lee, X. Feng, Y. Y. Huang, I. Adesida, R. G. Nuzzo, and J. A. Rogers, Nat. Mater. **5**, 33 (2006).
[13]A. Walther, *The Ray and Wave Theory of Lenses* (Cambridge University Press, Cambridge, 1995).
[14]P. Swain and D. Mark, Proc. SPIE **5499**, 281 (2004).
[15]T. Grayson, Proc. SPIE **4849**, 269 (2002).
[16]INSPEC, *Properties of Silicon* (Institution of Electrical Engineers, New York, 1998).
[17]See EPAPS supplementary material at http://dx.doi.org/10.1063/1.3256185 for finite element analysis.

Downloaded 09 Nov 2009 to 130.126.101.208. Redistribution subject to AIP license or copyright; see http://apl.aip.org/apl/copyright.jsp